Maximization of second-harmonic power using normal-cut nonlinear crystals in a high-enhancement external cavity

Yugo Onoda,[1,*] Michihiko Ikeda,[1] Kazuhiko Sugiyama,[1,2] Haruhisa Yokoyama,[1] and Masao Kitano[1,2]

[1]Graduate School of Electronic Science and Engineering, Kyoto University, Katsura, Nishikyo, Kyoto 615-8510, Japan

[2]Core Research for Evolutional Science and Technology, Japan Science and Technology Corporation, 4-1-8 Honcho Kawaguchi, Saitama, Japan

*Corresponding author: onoda@giga.kuee.kyoto-u.ac.jp

Received 22 August 2008; revised 18 November 2008; accepted 25 November 2008; posted 2 December 2008 (Doc. ID 100480); published 23 February 2009

When an antireflection-coated normal-cut nonlinear crystal is used in an external cavity for the generation of high second-harmonic power, a small residual reflection at the crystal facets causes a round-trip loss and prevents the realization of a large fundamental enhancement. This problem is eliminated when the reflected beams at the crystal facets are subject to constructive interference. We demonstrate that the temperature tuning of a β-BaB_2O_4 crystal of at most 3 K is sufficient to realize constructive interference at any wavelength. We achieve an enhancement factor of 125, and a second-harmonic power of 125 mW is generated at 398 nm from a fundamental power of 390 mW. © 2009 Optical Society of America

OCIS codes: 140.3515, 190.4360, 140.4780.

1. Introduction

Continuous-wave (CW) ultraviolet light sources are required in various fields, including high-resolution spectroscopy and laser cooling. For this purpose, second-harmonic generation (SHG) in nonlinear crystals has long been used. To increase the second-harmonic (SH) power, a nonlinear crystal is placed in an external cavity to enhance the fundamental power because of the low power of the beam from the CW laser [1]. Brewster-cut crystals [2,3] or antireflection (AR)-coated normal-cut crystals [4] are used in the external cavity. The former has the advantages that no loss is imposed by surface reflection and that the astigmatism and coma introduced at the Brewster-cut facets are compensated by the folding angle of the concave mirrors to focus the beam in the crystal [5]. The latter is also widely used because it is easier to align the ring cavity and the aberrations are small provided the folding angle is small.

When the finesse of an external cavity is sufficiently high to obtain a large fundamental enhancement factor, the enhancement factor is greatly affected by the round-trip loss. The small residual reflection at the crystal facets is one of the main causes of this loss when a normal-cut crystal is used, even though the crystal facets are AR-coated. The reflected beams from the two facets of the normal-cut crystal are subjected to interference, i.e., the crystal acts as an intracavity etalon. This shows that the loss imposed by the residual reflection at the crystal facets is eliminated when the reflected beams at the two facets are subjected to constructive interference. This technique is based on the theory of coupled cavity. Simultaneously, the interference causes the wavelength dependence of the enhancement factor, and the enhancement factor changes over long-time or day-to-day operation. In this paper, we discuss the effect of the small residual reflection at the crystal facets on the enhancement factor and the wavelength

0003-6935/09/071366-05$15.00/0

dependence of the enhancement factor. Although the effect of the residual reflection may be observed in other systems, no literature exists that discusses this problem to the best of our knowledge. To achieve constructive interference, i.e., the maximum enhancement factor at any wavelength, we demonstrate that temperature tuning is effective in our system containing a normal-cut β-BaB_2O_4 (BBO) crystal as a nonlinear crystal in an external cavity.

2. Theory

The fundamental enhancement factor A is described by

$$A = \frac{1-R}{\left(1-\sqrt{RV}\right)^2}, \tag{1}$$

where R is the input mirror reflectivity and the loss factor V is defined as $V = 1 - L$, where L is the fraction of the round-trip loss [1]. The linewidth of the fundamental laser is assumed to be narrower than the resonance width of the external cavity. Figure 1 depicts Eq. (1) to clarify the dependence of the enhancement factor A on V with the reflectivity of the input mirror R as a parameter. When R is high, a small difference in the intracavity loss markedly changes the enhancement factor. For example, for an external cavity with an input mirror of $R = 0.990$ and a fraction of round-trip loss of $L = 0.008$, one obtains $A = 125$. An increase in L of only 0.002, i.e., to 0.01, results in a decrease in A to 100. On the other hand, when $R = 0.950$, an increase in L of 0.002 only decreases A from 59 to 55. In addition, the SH power is proportional to the square of the enhancement factor. To achieve a high SH power by realizing a high-enhancement factor using a high-reflectivity input mirror, it is, therefore, essential to minimize the loss in the external cavity.

When one uses an AR-coated normal-cut nonlinear crystal in the external cavity, the residual reflection

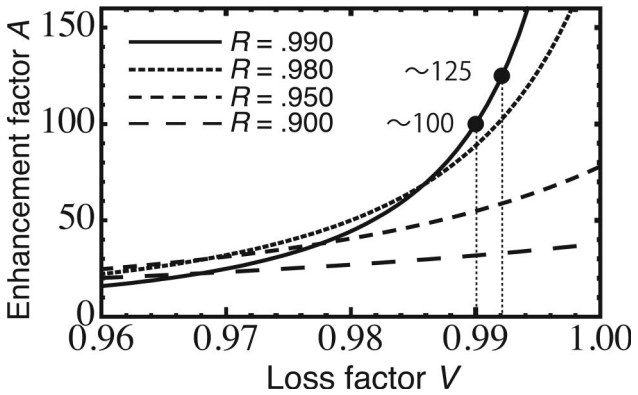

Fig. 1. Calculated enhancement factor A as a function of the loss factor V defined as $V = 1 - L$, where L is the fraction of the round-trip loss. When the reflectivity of the input mirror R is high (>0.98), the enhancement factor is strongly affected by the round-trip loss. For example, for $R = 0.990$, A decreases from 125 to 100 when L increases only by 0.002 from 0.008 to 0.010.

at the crystal facets is one possible loss factor. However, it is possible to eliminate the loss imposed by the residual reflection when the reflected beams from the two facets are subjected to constructive interference, i.e., the intracavity etalon composed of the residual reflection at the two crystal facets is resonant. The longitudinal mode spacing or free spectral range of a Fabry–Perot cavity in terms of wavelength $\Delta\lambda$ is given by

$$|\Delta\lambda| = \frac{\lambda^2}{2nl}, \tag{2}$$

where λ is the wavelength in vacuum, l is the distance between mirrors, and n is the refractive index of the material. We estimate $\Delta\lambda$ in our setup (see Section 3), which contains a 10 mm long BBO crystal, to be 0.019 nm for a fundamental wavelength of $\lambda = 798$ nm, where $n = 1.66$ for ordinary light at 798 nm [6]. This shows that the enhancement factor and, hence, the SH power, depends on the fundamental wavelength. It is desirable to achieve the maximum enhancement factor at any wavelength. For this purpose, the interference caused by the residual reflection at the two crystal facets must be tuned constructively. We investigate the temperature tuning of the optical path length of the cavity formed between the facets of the BBO crystal. In the worst case, temperature tuning is required to change the destructive interference to constructive interference. To realize this, the optical path length in the crystal is tuned by a quarter wavelength, with the change of the crystal temperature ΔT given by

$$\frac{d(nl)}{dT}\Delta T = \left(n\frac{dl}{dT} + l\frac{dn}{dT}\right)\Delta T = \frac{\lambda}{4}, \tag{3}$$

where T is the temperature of the crystal. We estimate ΔT for our BBO system. The thermo-optic coefficient dn/dT for ordinary light is -16.6×10^{-6}/K [7]. The thermal expansion coefficient, $(1/l)dl/dT = 28 \times 10^{-6}$/K at $\theta = 29.3°$, is derived from the equation $\alpha_a \sin^2\theta + \alpha_c \cos^2\theta$ [8] and the known values of α_a and α_c of 4×10^{-6}/K and 36×10^{-6}/K, respectively [7]. We find that a temperature change of 0.7 K is required to change the optical path length by $\lambda/4$, i.e., to tune the enhancement factor from the minimum to the maximum. The temperature tuning of a BBO crystal in an external cavity has also been applied to tune the resonance frequency of the external cavity to enable frequency scanning of a laser system [9].

3. Experimental Setup

Figure 2 shows a schematic diagram of the experimental setup. Radiation with a wavelength of 798 nm from a single-frequency CW titanium sapphire laser (Schwartz Electro-Optics Inc., Titan-CW. Two galvoplates and a galvo-driven thin etalon synchronously rotated with the galvoplates are introduced by us to enable frequency scanning.) is frequency doubled using a BBO crystal in an external cavity. The

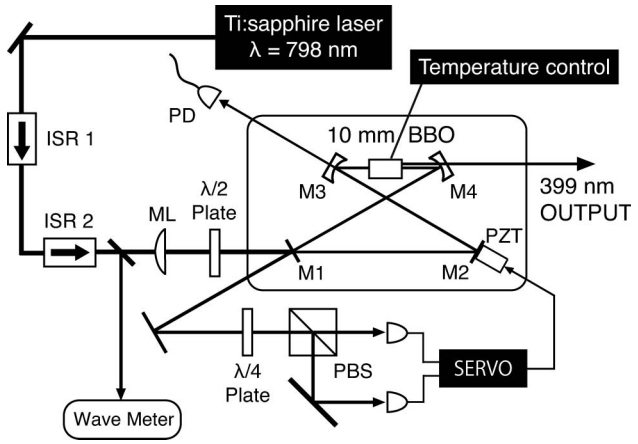

Fig. 2. Experimental setup. ISR, isolator; ML, mode-matching lens ($f = 750$ mm); M3, M4, concave mirrors with curvature radius of 50 mm; PZT, piezotransducer; PBS, polarizing beam splitter; and PD, photodiode. The PD is used to monitor the fundamental power inside the external cavity.

external cavity is composed of four mirrors in a bow-tie configuration. The total cavity length is approximately 400 mm, corresponding to a free spectral range of 750 MHz. The reflectivity of the input mirror R_{M1} is 0.990 ± 0.002, and those of the other mirrors R_{M2}, R_{M3}, and R_{M4} are more than 0.998 for the fundamental wavelength of 798 nm. The transmissivity of the output mirror M4 is 0.95 at 399 nm. To focus the fundamental beam in the BBO crystal, we use two concave mirrors with a curvature of 50 mm. The resonance frequency of the external cavity is locked to the frequency of the laser by controlling the cavity length using a piezotransducer (PZT) on which M2 is mounted. The frequency deviation from the cavity resonance is detected by a polarization spectroscopic method [10].

The BBO crystal is cut to $\theta = 29.3°$ to achieve Type-I phase matching to the normal incidence of the fundamental beam at 798 nm. The length of the crystal is 10 mm. The azimuth angle is cut to $\phi = 0°$ to maximize the nonlinear coefficient. The input and output facets are AR-coated for both fundamental and SH wavelengths. The parallelism of the crystal facets is 10″, which is the value in the standard specification of the crystal. The BBO crystal is placed in a holder made of copper, which is mounted on a Peltier element. The temperature of the copper holder, measured using a thermistor, is temperature controlled with a stability better than 0.01 °C (Thorlabs Inc., TED200C). Owing to the high finesse of the external cavity, a beam reversely propagating in the cavity is built up and fed back to the laser. This prevents electronic locking of the cavity resonance to the laser frequency. To avoid optical feedback, we inserted two isolators (Isowave, I-80T-5M) with isolation above 35 dB.

4. Results and Analysis

We measured the fundamental power built up in the external cavity and the SH power as a function of the fundamental wavelength, as shown in Fig. 3. We observed interference fringes in the fundamental power and the SH power synchronously changed in proportion to the square of the fundamental power. The pitch of the fringes was measured to be 0.019 nm. This value was in agreement with that obtained in Section 2. Therefore, we conclude that the fringes observed in Fig. 3 are caused by the residual reflection at the two facets of the BBO crystal.

We estimated the enhancement factor A by measuring the finesse of the external cavity. The finesse $\mathcal{F}$ is determined from the input mirror reflectivity R and the round-trip loss factor V by the following equation:

$$\mathcal{F} = \frac{\pi (RV)^{1/4}}{1 - \sqrt{RV}}. \tag{4}$$

One can determine the value of $\sqrt{RV}$, and then V, from the finesse $\mathcal{F}$. Then, the enhancement factor A can be estimated from Eq. (1). We measured the finesse by linearly scanning the frequency of the Ti:S laser by rotating the galvoplates inside the laser cavity. The finesse was determined to be 350 for the constructive interference and 310 for the destructive interference. From the reflectivity of the input mirror, $R_{M1} = 0.990 \pm 0.002$, the corresponding enhancement factors A were estimated to be 125 ± 25 and 100 ± 20, and the ratios of the round-trip loss L to be 0.008 ± 0.002 and 0.010 ± 0.002, respectively. The change in L shows that the residual reflectivity at the AR-coated crystal facet is approximately 0.001 for each facet.

Figure 4 shows the fundamental and SH powers measured by changing the crystal temperature. We again observed the same periodic change in the enhancement factor as that shown as a function of the wavelength in Fig. 3. The net optical path length nl in the crystal changed with its temperature and a temperature tuning of 3 K was required to change the destructive interference to constructive interference, or a half-cycle of the interference fringe in Fig. 4. This result is different from the theoretical

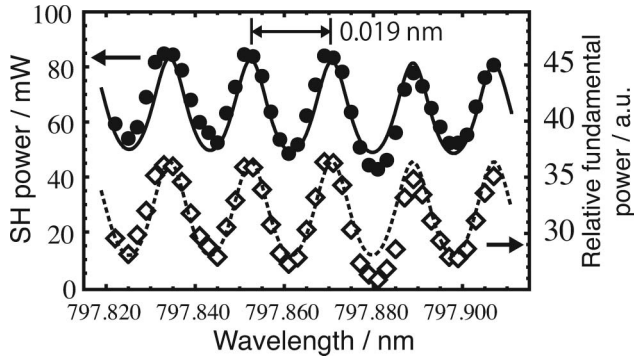

Fig. 3. Dependence of SH power (solid circles) and fundamental power (open diamonds) on the fundamental wavelength. The dashed curve is a Fabry–Perot function fitted to fundamental power. The solid curve is the square of the Fabry–Perot function fitted to SH power.

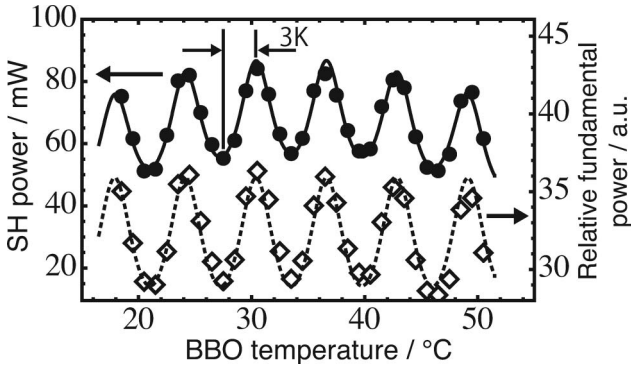

Fig. 4. Dependence of SH power (solid circles) and fundamental power (open diamonds) on temperature of BBO crystal. The dashed curve is a Fabry–Perot function fitted to the fundamental power. The solid curve is the square of the Fabry–Perot function fitted to the SH power. The decrease due to phase-mismatching expressed as the square of the sinc function is also included in the fitting.

estimation of 0.7 K obtained in Section 2. The reason for the discrepancy is not yet known. Assuming that the thermo-optic coefficient is correct, we estimate the value of $(1/l)dl/dT$ at 29.3° to be 14×10^{-6}/K.

When temperature tuning the interference fringe, it is important that the phase-mismatching tolerance in SHG is much larger than the tuning temperature for each half-cycle of the fringe. We define the phase-mismatching tolerance as the full width at half-maximum (FWHM) of a function $[\sin(\Delta kl/2)/(\Delta kl/2)]^2$, where Δk represents the phase mismatch. From the known parameters, we calculate the phase-mismatching tolerance to be 4.8 K. However, Fig. 4 shows that the effect of the phase-mismatching tolerance was negligible for tuning of 3 K. The observed phase-mismatching tolerance of approximately 50 K was much larger than the estimated value. The discrepancy is caused by the fact that the interaction length is shorter than the crystal length owing to the double refraction in the BBO crystal [11]. The interaction length, i.e., the aperture length, expressed as $l_a = \pi^{1/2}\omega_0/\rho$, was calculated to be 0.6 mm in our case, where ρ is the walk-off angle as described below. The FWHM phase-mismatching tolerance, derived using l_a instead of l, is 80 K. This is close to the experimental result. We measured the day-to-day reproducibility of the SH power at a fixed wavelength for one week; we switched the setup on and off every day, but the crystal temperature was continuously controlled for one week. A fluctuation of the SH power of 10% was detected, while 40% fluctuation was observed in the day-to-day operation without temperature control owing to the fluctuation of the ambient room temperature within approximately 2 °C.

When we tune the optical path length in the crystal to produce constructive interference, the reflection at the crystal facets is eliminated. Therefore, the backward beams in the external cavity and, hence, the optical feedback to the laser, are minimized. We achieved electronic locking of the cavity resonance to the laser frequency using only one isolator because of the reduced optical feedback. When we changed the crystal temperature by 0.7 K from that resulting in constructive interference, we found that a second isolator was necessary for stable frequency locking. Each isolator has an insertion loss of 11%. Therefore, the removal of one isolator has the benefit of increasing the fundamental power and hence the SH power.

The SH power generated under constructive interference is plotted in Fig. 5 as a function of the fundamental power. When the fundamental power in the crystal is depleted by conversion to the SH power and the absorption of the fundamental power and SH power in the crystal is negligible, the total conversion efficiency $\gamma_{\text{total}} = P_{2\omega}/P_{\omega}^2$, where P_{ω} and $P_{2\omega}$ are fundamental power and SH power, respectively, is expressed as

$$\gamma_{\text{total}} = \gamma_{\text{SHG}}\gamma_{\text{mm}}^2 A^2 = \gamma_{\text{mm}}^2 A^2 \frac{16\pi^2}{\epsilon_0 c\lambda_{\omega}^3}\frac{d_{\text{eff}}^2 l}{n^2} h(B,\xi), \quad (5)$$

where γ_{SHG} is the single-path conversion efficiency; γ_{mm} is the coupling or mode-matching efficiency of the fundamental beam to the external cavity; d_{eff} is the effective nonlinear coefficient; ϵ_0 is the electric constant; c is the vacuum speed of light; λ_{ω} is the fundamental wavelength in vacuum; n is the refractive index, which is the same for the fundamental and SH powers upon phase matching; $h(B,\xi)$ is the focusing function introduced by Boyd and Kleinman [12], where B is the double-refraction parameter defined as $B = \rho(k_{\omega}l)^{1/2}/2$, where ρ is the walk-off angle and k_{ω} is the propagation constant at the fundamental wavelength in the crystal; and ξ is the focusing parameter defined as $\xi = l/b$, where $b = w_0^2 k_{\omega}$ is the confocal parameter and w_0 is the radius of the fundamental beam at focus. Our external cavity is designed so that $\xi = 1.39$. The walk-off angle ρ of

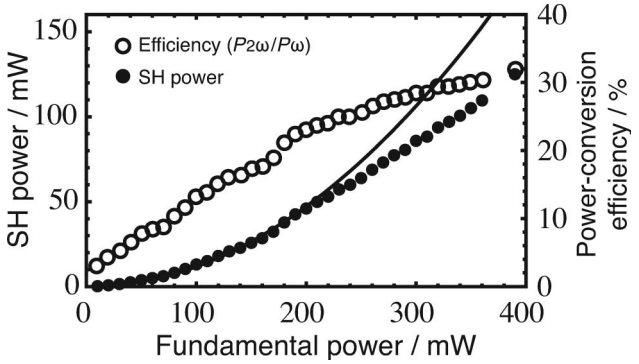

Fig. 5. SH power and corresponding power-conversion efficiency $P_{2\omega}/P_{\omega}$ as a function of the fundamental power when the fundamental enhancement factor is maximized by temperature tuning, where P_{ω} and $P_{2\omega}$ are the fundamental and SH powers, respectively. The solid curve represents the calculated SH power assuming no depletion of the fundamental power by conversion to the SH power. The calculated parameters are given in the text. The highest SH power of 125 mW was achieved at a fundamental power of 390 mW.

68 mrad, calculated from the known parameters [13], leads to $B = 12$. Then, we estimate the value of h to be 0.058. We calculate d_{eff} to be 1.9 pm/V from the equation $d_{\mathrm{eff}} = d_{31}\sin(\theta+\rho) + d_{22}\cos(\theta+\rho)$ and the known values of the coefficients [14]. We estimate γ_{SHG} to be 0.93×10^{-4}/W. We experimentally determined the value of γ_{mm} to be 0.9. Finally, when we assume that $R_{\mathrm{M1}} = 0.990$, i.e., $A = 125$ for the constructive interference, we estimate γ_{total} to be 1.2/W. This value is in good agreement with the results shown in Fig. 5; in the region of low power-conversion efficiency ($P_{2\omega}/P_{\omega}$) is below 15%. The conversion efficiency is similar to that obtained using a Brewster-cut BBO crystal [2,3]. The discrepancy compared with the estimated conversion efficiency in the high power-conversion efficiency region of over 15% is caused by the depletion of the fundamental power by conversion to the SH power [15].

5. Conclusion

We have demonstrated that the small residual surface reflection at the facets of a normal-cut nonlinear crystal markedly decreases the enhancement factor when the external cavity has high finesse. We propose that this problem is eliminated when the beams reflected at the two facets are subjected to constructive interference and we demonstrate a solution to the problem by temperature tuning of the BBO crystal used in our setup. A temperature change of at most 3 K is sufficient to achieve the maximum enhancement factor at any wavelength and this tuning range is much smaller than the phase-mismatching tolerance of the temperature. The method of temperature tuning to maximize the enhancement factor can be applied to an external cavity with other materials used as a nonlinear crystal. For example, with a 10 mm long normal-cut LBO crystal for SHG at 798 nm, we estimate that a temperature change of at most 0.3 K could maximize the enhancement factor according to our calculation for the BBO crystal. A different tuning method, such as electronic tuning using an electro-optic effect, may also be feasible.

This work was partly supported by the Grant-in-Aid for Scientific Research (No. 20.6222) and by the Global Center of Excellence program from the Japan Society for the Promotion of Science (JSPS).

References

1. M. Brieger, H. Büsener, A. Hese, F. V. Moers, and A. Renn, "Enhancement of single frequency SGH in passive ring resonator," Opt. Commun. **38**, 423–426 (1981).
2. B. Beier, D. Woll, M. Scheidt, K. J. Boller, and R. Wallenstein, "Second harmonic generation of the output of an AlGaAs diode oscillator amplifier system in critically phase matched LiB_3O_5 and β-BaB_2O_4," Appl. Phys. Lett. **71**, 315–317 (1997).
3. J. D. Bhawalkar, Y. Mao, H. Po, A. K. Goyal, P. Gvrilovic, Y. Conturie, and S. Singh, "High-power 390 nm laser source based on efficient frequency doubling of a tapered diode laser in an external resonant cavity," Opt. Lett. **24**, 823–825 (1999).
4. H. Kumagai, Y. Asakawa, T. Iwane, K. Midorikawa, and M. Obara, "Efficient frequency doubling of 1-W continuous-wave Ti:sapphire laser with a robust high-finesse external cavity," Appl. Opt. **42**, 1036–1039 (2003).
5. M. H. Dunn and A. I. Ferguson, "Coma compensation in off-axis laser resonators," Opt. Commun. **20**, 214–219 (1977).
6. K. Kato, "Second-harmonic generation to 2048 Å in β-BaB_2O_4," IEEE J. Quantum Electron. **22**, 1013–1014 (1986).
7. D. Eimerl, L. Davis, and S. Velsko, "Optical, mechanical, and thermal properties of barium borate," J. Appl. Phys. **62**, 1968–1983 (1987).
8. S. K. Filatov, N. V. Nikolaeva, R. S. Bubnova, and I. G. Polyakova, "Thermal expansion of β-BaB_2O_4 and BaB_4O_7 borates," Glass Phys. Chem. **32**, 471–478 (2006).
9. H. Kumagai, "Fine frequency tuning in sum-frequency generation of continuous-wave single-frequency coherent light at 252 nm with dual-wavelength enhancement," Opt. Lett. **32**, 62–64 (2007).
10. T. W. Hänsch and B. Couillaud, "Laser frequency stabilization by polarization spectroscopy of a reflecting reference cavity," Opt. Commun. **35**, 441–444 (1980).
11. K. Sugiyama, J. Yoda, and T. Sakurai, "Generation of continuous-wave ultraviolet light by sum-frequency mixing of diode-laser and argon-ion-laser radiation in β-BaB_2O_4," Opt. Lett. **16**, 449–451 (1991).
12. G. D. Boyd and D. A. Kleinman, "Parametric interaction of focused Gaussian light beams," J. Appl. Phys. **39**, 3597–3639 (1968).
13. T. Freegarde and J. Coutts, "General analysis of type I second-harmonic generation with elliptical Gaussian beams," J. Opt. Soc. Am. B **14**, 2010–2016 (1997).
14. I. Shoji, H. Nakamura, K. Ohdaira, T. Kondo, and R. Ito, "Absolute measurement of second-order nonlinear-optical coefficients of β-BaB_2O_4 for visible to ultraviolet second-harmonic wavelengths," J. Opt. Soc. Am. B **16**, 620–624 (1999).
15. K. R. Parameswaran, J. R. Kurz, R. V. Roussev, and M. M. Fejer, "Observation of 99% pump depletion in single-pass second-harmonic generation in a periodically poled lithium niobate waveguide," Opt. Lett. **27**, 43–45 (2002).